ASSESSMENT OF RESIDUAL GEOGENIC CARBON IN MORTARS CONCERNING RADIOCARBON DATING

Jan Válek[1]* • Petr Kozlovcev[1] • Anna Fialová[1] • Kristýna Kotková[1] • Dita Frankeová[1] • Ivo Světlík[2] • Kateřina Pachnerová Brabcová[2]

[1]Institute of Theoretical and Applied Mechanics of the Czech Academy of Sciences, Prosecká 809/76, 190 00 Praha, Czech Republic
[2]Department of Radiation Dosimetry, Nuclear Physics Institute of the Czech Academy of Sciences, Na Truhlářce 39/64, 180 00 Praha, Czech Republic

ABSTRACT. Quicklime samples were collected from six vertical layers (L1–L6) of a feedstock calcined in a traditional single-batch wood-fired kiln and assessed. Three samples were well-burned and three under-burned. The quicklime was slaked in an excess of water and the presence of unburned particles was investigated after settling it into putty. The putty was assessed as bulk and also at three depth levels. Thermal analysis determined the CO_2 residua in the quicklime samples. Cathodoluminescence detected individual unburned particles and image analysis was used for their quantification. Settling of the putties led to a considerable reduction of geogenic particles in the layers above the bottom. This was also confirmed by the stable isotope analysis. In the case of the putties made from well-burned quicklime, the $\delta^{13}C$ values of samples L4 and L5 ranged from –25.5‰ to –20.5‰ VPDB, and the $\delta^{18}O$ values ranged from –17.5‰ to –16.5‰ VPDB. The fractionation was likely affected by the division according to the particle size during the sedimentation. The results of the ^{14}C analysis correlate with the quantified percentage of cathodoluminescent particles.

KEYWORDS: C and O stable isotopes, cathodoluminescence, lime binder, lime processing.

INTRODUCTION

Lime mortars are an important source of knowledge about historic buildings. Their characterization can provide information on the composition and quality of raw materials and construction technologies. Lime binders harden by absorption of atmospheric CO_2, which makes them a promising material for radiocarbon dating (Labeyrie and Delibrias 1964; Stuiver and Smith 1965; Baxter and Walton 1970; Lindroos et al. 2018; Hajdas et al. 2020; Daugbjerg et al. 2021). Several published articles prove that lime mortars can be successfully used to establish absolute chronology and provide information about the building history of a site (Addis et al. 2019; Hajdas et al. 2012; Heinemeier et al. 2010; Nawrocka et al. 2009; Ortega et al. 2012; Ringbom et al. 2014; Van Strydonck 2016; Caroselli et al. 2020). However, there are also well-known obstacles that affect radiocarbon dating and its potential to provide conclusive results.

In addition to CO_2 absorbed by carbonation (so-called anthropogenic carbon), which carries the coeval atmospheric ^{14}C, historic lime binders contain contaminants. According to the type, contaminants can lead to the aging and/or rejuvenation of the dated mortars. The aging is caused by the presence of fossil carbonates that contain geogenic carbon (Lindroos et al. 2007; Ponce-Antón et al. 2018). Typically, aggregate and filler can contain carbonates. Their sizes are usually in the range of tens of microns to units of millimeters and thus such contaminants can be in principle detected by a petrographic analysis in an optical microscope. An additional important source of contamination is an ineffective production or insufficient technological processing of lime binder. The burning conditions in the lime kiln cause some of the raw material may not fully calcine. In wood-fired single-batch kilns, which were the most commonly spread types from antiquities (and earlier) to modern times, the burning conditions were very heterogeneous (Wingate 1985; Adam 1994; Válek 2015). The geogenic carbon would

*Corresponding author. Email: valek@itam.cas.cz

thus be a common part of every lime batch produced. However, this source of contamination was likely to be highly variable as it was linked to a human factor.

Quicklime is processed into a binder by slaking (Oates 1998). Calcium oxide exothermically reacts with water to form calcium hydroxide. The reaction disintegrates calcium oxide into fine particles ranging approximately from 1 to 200 μm and larger. Under-burned quicklime particles are composed of three phases, an unburned limestone core, a partially calcined transitional zone, and fully calcined lime (Kozlovcev and Válek 2021). Both the core and transitional zone contain remnants of the raw material and thus also geogenic carbon. The core does not react during slaking but the partially calcined material disintegrates into smaller particles. The actual content of geogenic carbon in lime mortars depends on a specific way of binder processing. One of the traditional methods of slaking was to use excess water to form a lime putty. Slaked putty was left to settle in a lime pit before its usage (Cazalla et al. 2000).

Assessment of the presence of particles containing geogenic carbonate is of utmost importance for radiocarbon dating of historic lime binders. Two methods are known, the cathodoluminescence microscopy (CL) and the stable isotopes $\delta^{13}C$ and $\delta^{18}O$ determination (Addis et al. 2019; Ricci et al. 2022). The CL can be used to identify natural carbonates (and also unburnt particles in binder) and it is considered suitable for distinguishing the presence of limestone in a historic binder (Toffolo et al. 2019).

The fractionation of stable carbon and oxygen isotopes has been shown to indicate the atmospheric CO_2 and water content during carbonation (Pachiaudi et al. 1986, Letolle et al. 1992). The lighter isotopes ^{12}C and ^{16}O are enriched vs. ^{13}C and ^{18}O compared to atmospheric CO_2 from which the precipitated calcium carbonate is formed. The fractionation mechanism relates to an alkaline environment (high pH) caused by the reacting calcium hydroxide. According to Kosednar-Legenstein et al. (2008), the isotope fractionation coefficient between the precipitated calcite and gaseous CO_2 $\Delta^{13}C_{Calcite-CO2}$ is –18‰. Considering the isotope composition of the Earth's atmosphere during the last two thousand years, the $\delta^{13}C$ and $\delta^{18}O$ for precipitated calcite can be expected about –24‰ to –27‰ and –18‰ to –22‰ VPDB (Vienna Pee Dee Belemnite), respectively (Kosednar-Legenstein et al. 2008). However, the isotope fractionation coefficient $\Delta^{13}C_{Calcite-CO2}$ decreases to –13‰ at lower pH (< 9.5) (Usdowski and Hirschfeld 2000) and specific carbonation conditions seem to affect the resulting isotopic composition.

The aim of this work is to assess the amount of unburned particles in a traditionally prepared lime binder and to evaluate two known assessment methods, cathodoluminescence microscopy and determination of stable isotope composition after mortar carbonation.

MATERIALS AND METHODS

Lime Samples

The experiment aimed to assess the presence of particles containing geogenic carbon in lime binder produced in a single-batch wood-fired lime kiln and slaked in excess of water into lime putty.

A suitable material was obtained by calcination of high calcium limestone (CaO 55.5%, MgO 0.3%, based on XRF analysis provided by the supplying quarry), in an experimental lime kiln replicating the historical wood-fired single batch process (Válek 2015). The quicklime was divided horizontally into six layers based on the assumption of the degree of calcination (Figure 1; Table 1). Each layer was taken out separately, placed on a platform, and assessed. It

Table 1 Estimation of residual geogenic CO_2 (% w/w) in quicklime from the different kiln positions.

Sample	Sample position	Quality of lime	CO_2 geogenic residue	$CaCO_3$ geogenic
L1	Top 30 cm, the upper part	Macroscopically visible unburned cores—under-burned lime.	23.83*	54.2
L2	Top 30 cm, the middle part		10.9*	24.8
L3	Top 30 cm, the lower part		7.4*	16.8
L4	Middle of the kiln	Well-burned lime	0.19	0.4
L5	Middle of the kiln	Well-burned lime	0.0	0.0
L6	Around the combustion chamber	Well-burned lime with some unburned material	3.59	8.2

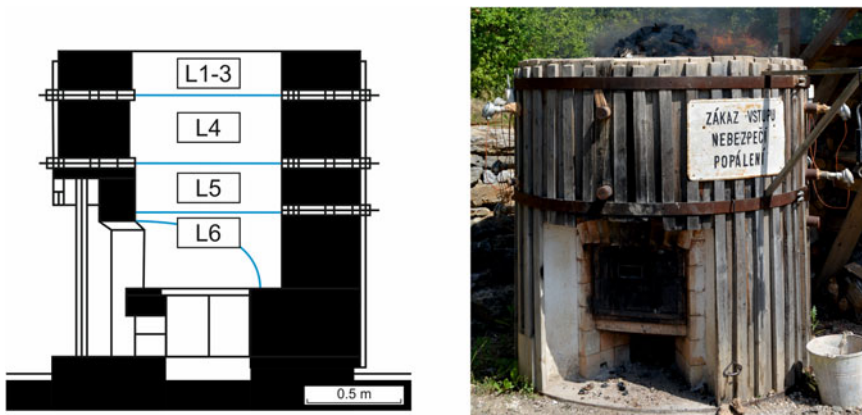*Estimated based on thermogravimetric analysis of spot samples.

Figure 1 View and cross-section of the single batch wood-fired experimental lime kiln. The height of the kiln is 1.8 m, and one fill is approximately 800 kg of limestone. Samples of quicklime were taken from layers L1 to L6.

was based on visual appearance (color change) and an estimation of the weight of pieces (unburned stones are notably heavier for their size). The top three layers L1–L3 showed a high portion of under-burned lime. To use this material as a binder it had to be slaked first to separate the reactive material from the unburned cores. This was regarded as the only practical way how to obtain a representative sample of a slaked lime from this very heterogeneous mixture.

However, the quicklime from layers L4–L6 seemed well-burned (only later, the analysis revealed that layer L6 comprised some under-burned material, probably from the very bottom of the kiln). The quicklime from each of these three layers was mixed and a representative sample of approximately 0.6 kg was taken and stored in vacuum-sealed containers before further processing. Since these samples were considered well-burned, carrying out a standard reactivity test (EN 459-1 2015) on them was possible to obtain additional characterizing parameters. The test itself also provides the same slaking conditions, which means better comparability of the resulting lime putties.

The slaked lime from all six kiln layers was left to settle in glass beakers in the laboratory and sampled for further analysis at the maturation age of 7 days. Sampling was carried out in vertical profiles by dipping a glass tube directly to the bottom. The tube was closed with a thumb at the end and the bulk sample was taken out. Another sample was taken and divided into three parts representing the surface, middle, and bottom of the beaker. The samples were placed on Petri dishes and were left to carbonate under standard laboratory conditions for three months. A phenolphthalein pH indicator was used to confirm their full carbonation. These samples were studied employing cathodoluminescence microscopy, stable isotopes ^{13}C and ^{18}O content and finally, ^{14}C analysis was carried out.

Methods

Traditional Slaking and Sampling of Slaked Lime
The quicklime from layers L1–3 was individually slaked in excess of water in a wooden slaking vessel following the traditional process. The ratio of quicklime to water was approximately 1:5 by volume. Water was added in steps, approximately 50% at the beginning, and the rest within the first minute when the reaction started. The lime milk obtained was left to stand for half an hour with occasional stirring and then passed through a 4 mm sieve to a lime pit. Spot samples of sieved lime milk of approximately 1 l were taken.

Laboratory Slaking and Reactivity (R)
The EN 459-2 reactivity test was carried out to compare the properties of well-burnt quicklime samples L4–6. A quantity of 450 g of each quicklime was crushed to produce a 150 g fraction passing a 2 mm sieve. The quicklime was added to a Dewar vessel containing 600 ml of distilled water (± 20°C). The vessel was equipped with a stirring paddle (set at ± 300 RPM) and a digital thermometer connected to a data logger. The temperature was measured at 30 s intervals for 2 hr. The test was repeated three times for each sample. The lime milk produced in the first rounds of the test was taken as a sample for further studies.

Thermal Analysis (TA)
The instrument SDT Q600 (TA Instruments) was used to measure thermal behavior between 25 °C and 1000 °C for which a sample of approximately 10 mg was heated at the rate of 20 °C/min in air and/or in a nitrogen atmosphere. The quicklime samples were stored in vacuum-sealed containers and were homogenized and ground with a pestle in a mortar before analysis.

X-ray Diffraction (XRD)
Samples were homogenized and data were collected on a diffractometer D8 Bruker Advance pro (Cu Ká radiation, 40kV and 40mA) with 0.01°C step size 2Ө and counting time 0.4 s/step.

Optical Microscopy (OM) and Cathodoluminescence (CL)
Samples for optical microscopy (OM) and observation of the cathodoluminescence (CL) were prepared as follows: the material, i.e., dried/carbonated lime putty, was at first crushed in an agate bowl; subsequently, 0.1 g of material was weighed and evenly imposed onto a standard thin-section glass. Through this process, a uniform layer of material was retrieved. The samples were observed using an Olympus BX53M conventional optical/polarizing microscope coupled with a "cold" cathode CITL type CCI 8200 Mk4. The measurement conditions were as follows: beam current 250 lA, electron energy 14–16 kV. Images were taken by DP74 digital camera with exposure time set to 30 s.

Quantitative phase analysis (QPA) of luminescent particles was performed by Stream Essentials Olympus software. QPA analysis was based on the detection of RGB spectra of the acquired image and concerned two groups of luminescent particles, the bright particles with the red compound from 140 to 256 (RGB: R=140–256; G=0; B=0) and the dull/diffuse particles with the red color compound from 80 to 140 (RGB: R=80–140; G=0; B=0). The results of QPA are presented as an average percentage of luminescent particles in observed areas of five different microscope view fields.

Stable Isotopes by Mass Spectroscopy

The carbonated putty samples (about 16 to 20 mg) were decomposed by 100% H_3PO_4 under a vacuum at 25°C (McCrea 1950). The carbon and oxygen isotopic composition of the evolved CO_2 gas was measured using a DeltaV Advantage IRMS (Delta V Isotope Ratio Mass Spectrometer), Dual Inlet, in the Laboratories of the Czech Geological Survey in Prague. Results are displayed using the usual δ notation related to Vienna Pee Dee Belemnite (VPDB). The analytical error was ±0.1‰ for both $\delta^{13}C$ and $\delta^{18}O$ values. The accuracy of the measurement was checked by analyses of the international standard (IAEA) NBS 18 ($\delta^{13}C = -5.014$‰, $\delta^{18}O = -23.2$‰) and two in-house standards: Carrara marble ($\delta^{13}C = 2.29$‰, $\delta^{18}O = -1.32$‰) and CS 2 ($\delta^{13}C = 2.93$‰, $\delta^{18}O = -3.86$‰). The long-term reproducibility for all standards is better than 0.05‰ for $\delta^{13}C$ and 0.1 for $\delta^{18}O$.

Radiocarbon Analysis by AMS

The samples (about 5 mg) were digested by exposure to concentrated H_3PO_4 in an evacuated glass reactor, with a volume of about 6 mL. The resulting CO_2 was cryogenically isolated and reduced to graphite with Zn and Fe as catalysts (Orsowszki and Rinyu 2015). The graphite samples were pressed into aluminum cathodes and measured with accelerator mass spectrometry (AMS) system MILEA at the Nuclear Physics Institute of the CAS (lab code CRL) or MICADAS at Hertelendi Laboratory of Environmental Studies in Hungary (lab code DeA) together with radiocarbon Standard Reference Material (oxalic acid II, NIST SRM 4990C) and blank material (anhydride of phthalic acid). The AMS data were processed with BATS software (Wacker et al. 2010).

RESULTS AND DISCUSSION

Determination of Geogenic CO_2 Residue in Quicklime by TA

The macroscopic observation and subsequent TA analysis confirmed that the three upper layers were considerably under-burned (see Table 1). The proportion of calcium carbonate, containing geogenic carbon remaining in quicklime in layers L1–L3, was approximately 16–55% (w/w). The analysis was carried out on spot samples, which were drilled cylindrical cores (50 mm in diameter and 50 mm long), placed in the kiln as controls near thermocouples monitoring temperatures during the burning process.

TA analysis of the representative samples from the L4 and L5 layers indicated that lime from the central part of the kiln was well-burned with minimum geogenic CO_2 residue (< 0.5 % w/w). Layer L6 was considered as well-burned and thus treated the same way as layers L4 and L5 but the TA analysis revealed the presence of under-burned material.

The thermal analysis quantified the amount of residual CO_2 in the produced quicklime. Two distinct processes took place in the temperature range of carbonate decomposition (Cizer Ö et al. 2012) and were described as types I and II, see Figure 2. Type I (temperature range 500 to
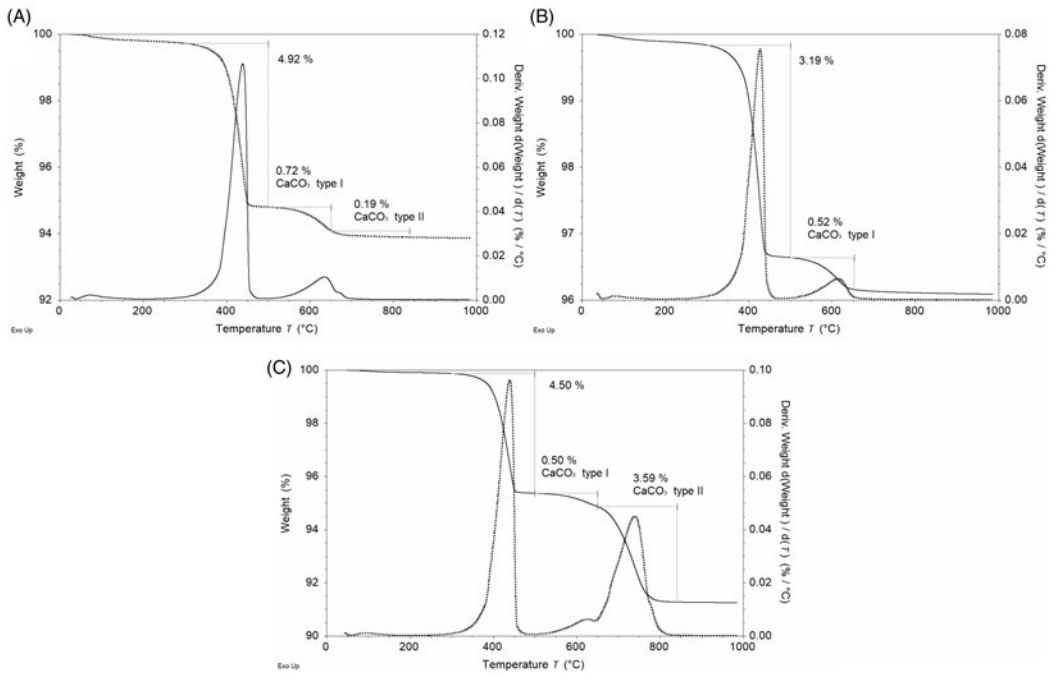
Figure 2   TG (solid) and DTG (dotted) curves of the L4 (A), L5 (B), and L6 (C) samples. All three samples contain portlandite (around 425°C). Samples L4 and L6 show two distinct processes in the temperature range from 500°C to 850°C. Sample L5 contains only carbonate that decomposes in the temperature range from 500°C to 650°C.

650 °C) was associated with the newly formed calcium carbonate, and type II with the geogenic residue. The decomposition of both $CaCO_3$ types is visible on samples L4 and L6. Sample L5 does not contain any carbonate type II that would decompose above 650°C so it was assumed to be fully burned without any geogenic CO_2 residue. To quantify the $CaCO_3$ type II the temperature range from 650 to 850 °C was applied.

All quicklime samples studied contained calcium hydroxide and $CaCO_3$ type I, even though they were kept in airtight containers. The hydration by atmospheric humidity and subsequent carbonation most likely occurred on the surface of quicklime particles during the cooling phase in the kiln and the handling of the samples. $CaCO_3$ type I was formed under different conditions than it would in a mortar as a binder. XRD analysis showed a presence of calcite, quicklime, and portlandite but no phase modifications of $CaCO_3$ were detected. The possibility to distinguish the $CaCO_3$ types I and II seems limited to freshly carbonated quicklime, it is not observable in carbonated historic mortars (Frankeová and Koudelková 2020).

Assessment of Unburned Particles in Carbonated Lime Putty by CL

All carbonated putty samples comprised a certain proportion of red luminescent particles related to geogenic remains. However, there were notable differences between the two sets, the under-burned layers L1–L3 and the well-burned layers L4–6, see Figure 3 and Table 2. The red luminescent particles were much more abundant in the under-burned lime putties. The size of particles was most often in the range of 5–20 μm and the largest particles were almost 50 μm in

Table 2   Quantification of luminescent geogenic carbonate particles (red luminescence). The values represent the average percentage of luminescent particles and the standard deviation (in brackets).

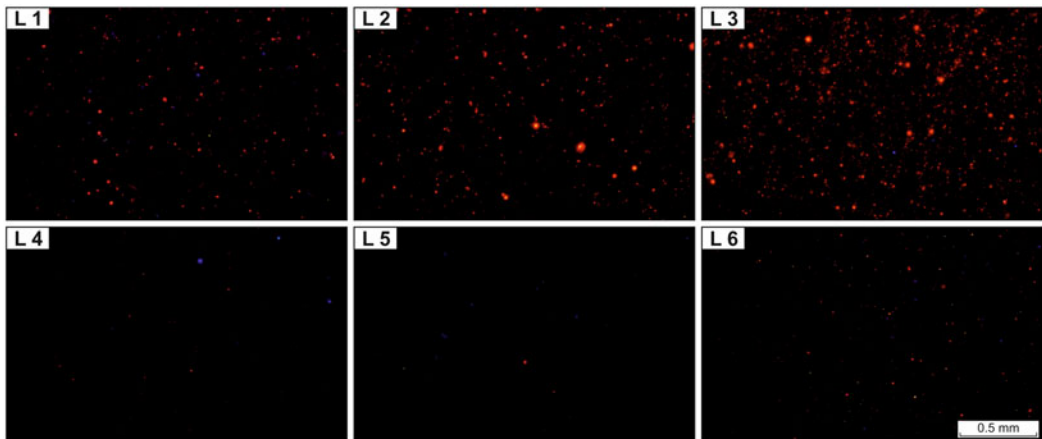| Luminescent particles	Interval of red spectrum RGB (G = 0; B = 0)	L1	L2	L3	L4	L5	L6
Bright	R = 150–256	0.75	0.96	1.87	0.01	0.00	0.13
Dull	R = 80–150	3.23	3.86	13.97	0.04	0.02	0.80
		3.98	4.80	15.84	0.05	0.02	0.93
All	R = 80–256	(0.50)	(0.66)	(1.21)	(0.01)	(0.02)	(0.18)

Figure 3   Comparison of luminescent particles in the carbonated lime putty samples L1–L6.

diameter. Larger particles than that were not retained due to sample preparation. The well-burned samples L4 and L5 comprised very few luminescent particles.

The luminescence color used to determine the percentage of particles differed. The brightest particles were assumed to be in the upper part (on or close to the surface) of the sample. The dull and also slightly blurred and foggy particles were probably from deeper positions within the sample, see Table 2.

The effect of sedimentation on the presence of luminescent particles was observed on the samples taken in the vertical profile. In general, all samples from the surface and middle layers contained significantly fewer red luminescent particles, if any, than the samples from the bottom layer. This was best observed on the most "contaminated" sample L3 (see Figure 4).

The CL assessment confirmed a higher amount of under-burned particles in the L1–L3 samples compared to the L4–L6 samples. The under-burned particles were the most abundant in sample L3. The image analysis quantification of samples L4–L6 agrees with the TA results of the quicklime samples. Heavier under-burned particles settled faster, and this process significantly reduced their presence in the volume above the bottom.
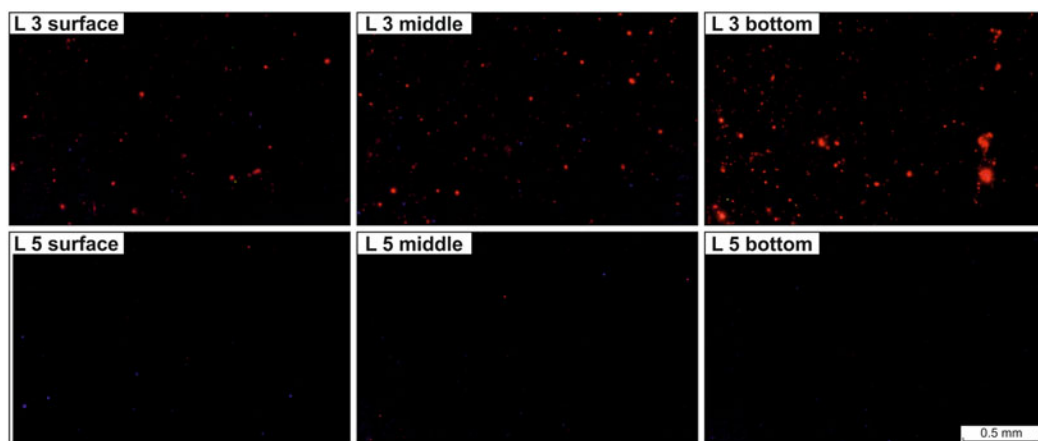
Figure 4   Comparison of luminescent particles present in the carbonated lime putty samples L3 and L5. Samples L5 show almost no luminescent particles.

Stable Isotopes Composition of Carbonated Lime Putty

All carbonated putty samples comprised newly precipitated calcium carbonate as a major component and various amounts of unburned limestone residues. The fractionation of the stable isotopes ^{13}C and ^{18}O reflected this composition (Table 3). The δ^{13}C and δ^{18}O values of carbonated bulk samples L4–L6 were around –21‰ and –14.5‰ VPDB (Vienna Pee Dee Belemnite), the samples L1–L3 had these values shifted towards heavier isotopes by the residues of the un-burned limestone (Dotsika 2009).

According to Kosednar-Legenstein et al. (2008), recently precipitated calcium carbonate by atmospheric CO_2 should have δ^{13}C around –25‰ VPDB and δ^{18}O around –20‰ VPDB considering the reaction takes place by absorption of atmospheric CO_2 in an ideal matrix layer. The authors also experimentally demonstrated that there is a continuous enrichment of ^{13}C vs. ^{12}C of the calcite precipitated by absorption of CO_2 with increasing depth of the material, i.e., the interior of a mortar layer is isotopically heavier compared to the exterior. In addition, there was a positive correlation between δ^{13}C and δ^{18}O isotopes which they defined by the equation:

$$\delta^{18}O = 0.67 \times \delta^{13}C - 6.4 \tag{1}$$

This correlation has a very similar slope with a line drawn between the isotope values of precipitated calcite in the ideal layer discussed above and the limestone used in the experiment (Figure 5).

The δ^{13}C and δ^{18}O values of the carbonated putties L1–L6 do not indicate any strong correlation. When split into two groups, the isotope values of samples L1–L3 follow approximately the line that connects the calcite from the ideal matrix layer and the limestone isotopes. The δ^{13}C and δ^{18}O values of samples L4–L6 are close together. However, their location does not correspond to the expected fractionation of the calcite precipitated in the ideal matrix layer.

A positive effect of the settling of lime putty on the separation of unburned particles can be observed as the bottom samples of the L1–3 putties are those that are isotopically heavier.

Table 3   Stable isotope $\delta^{13}C$ and $\delta^{18}O$ values in raw material and carbonated lime putty samples L1–L6. For the putties, values are given for the whole bulk and the parts representing the surface (S), middle (M), and bottom (B) sections of the vertical profile.

		$\delta^{13}C$ (‰ VPDB)	$\delta^{18}O$ (‰ VPDB)
Limestone samples 1–3	1	2.9	–3.1
	2	2.8	–3.2
	3	2.8	–3.0
Carbonated putty samples L1–L6 (bulks)	L1	–18.0	–14.8
	L2	–17.4	–15.0
	L3	–14.5	–13.4
	L4	–20.7	–14.1
	L5	–20.3	–14.6
	L6	–21.2	–15.0
Carbonated putty L1 (profile)	S	–22.8	–16.6
	M	–22.4	–16.7
	B	–20.1	–15.7
Carbonated putty L2 (profile)	S	–22.9	–16.7
	M	–22.8	–16.6
	B	–19.9	–15.5
Carbonated putty L3 (profile)	S	–22.4	–16.3
	M	–21.5	–16.2
	B	–18.8	–15.1
Carbonated putty L4 (profile)	S	–24.3	–16.7
	M	–25.6	–16.5
	B	–25.5	–16.9
Carbonated putty L5 (profile)	S	–21.7	–17.2
	M	–20.5	–17.5
	B	–21.3	–17.5
Carbonated putty L6 (profile)	S	–22.0	–16.9
	M	–22.3	–17.5
	B	–23.0	–18.0

The division of the putty samples into the surface, medium, and bottom parts shows that the geogenic residue shifts the values towards the heavier isotopes along the line connecting the calcite precipitated in the ideal matrix layer and the raw material isotopes. In the case of the putties made from well-burned quicklimes, the $\delta^{13}C$ values of samples L4 and L5 range from –25.5‰ to –20.5‰ VPDB, and the $\delta^{18}O$ values range from –17.5‰ to –16.5‰ VPDB (Figure 5). (Note, sample L6 is considered as well-burned lime but the TA assessment showed some residual CO_2 in the quicklime, so it was not included in this range.) The isotopic fractionation is not uniform although the samples were cured under the same conditions. It seems that some additional factors affect the fractionation of the isotopes. All the surface samples are closer to each other than those of the bottom or middle positions. This also regards the surface samples of putties L1–L3. It seems that the fractionation of stable isotopes $\delta^{13}C$ and $\delta^{18}O$ of precipitated calcium carbonate is affected by the character of calcium hydroxide particles. Gravitational settling is a well-known mechanism for sorting lime particle sizes in a vertical profile. The finest particles are expected near the surface, the coarsest particles are at the bottom. The surface and, to a certain extent, the middle part of the settled putties L1–L6 consisted of calcium hydroxide/calcium carbonate with zero or minimum geogenic residues.
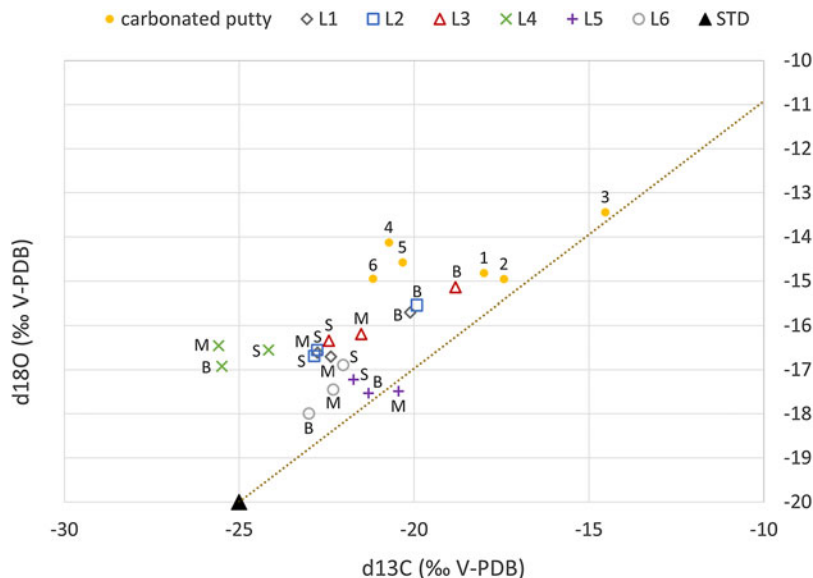
Figure 5   Stable C and O isotope values of the precipitated calcite in bulk (L1–L6) and three vertical sections (S, M, B) of putty samples. The line connecting the isotope values of precipitated calcite in the ideal matrix layer (STD calcite [$\delta^{13}C = -25‰$ VPDB; $\delta^{18}O = -20‰$ VPDB]) and the limestone used in the experiment (STD limestone [$\delta^{13}C = 2.9‰$ VPDB; $\delta^{18}O = -3.1‰$ VPDB]) has a slope of 0.605.

There, the isotopic fractionation was mainly affected by the conditions of the carbonation reaction (Usdowski 1982; Usdowski and Hirschfeld 2000). The bottom parts of lime putties L1–L3 contained some unburned particles with geogenic CO_2 residues that influenced the isotope values. The calcium hydroxide was, however, the main compound that determined the final isotopic composition.

Compared to CL, stable isotope values cannot detect the small number of unburned materials in a sample composed mostly of newly precipitated calcite. However, a value of $\delta^{13}C \geq -20.0$ ‰ VPDB can be considered to indicate a significant presence of geogenic carbon. Such samples should not be used for radiocarbon dating. This is in agreement with recommendations in the literature based on the evaluation of historic mortars (Dotsika 2009; Hayen et al. 2017; Ricci et al. 2022).

Radiocarbon Analysis

Activities of ^{14}C expressed as conventional radiocarbon age (CRA) in years before present (BP) (Stuvier and Polach 1977) for the carbonated lime putty samples L1–L6 are summarized in Table 4. CRA ages linearly correlate with CL all luminescent particles expressed as % of the area (intercept 103.68 ± 19.17, slope 160.47 ± 2.45), with Pearson's correlation coefficient of 0.9982.

Traditional Lime Burning Process and Its Impact on Mortar Dating

The experiment demonstrates that lime burned in a wood-fired flare kiln is likely to contain some geogenic CO_2. This is a specific source of contamination that can cause errors in radiocarbon dating of the binder. The particles containing geogenic carbon can be expected to

Table 4   The activity of ^{14}C for carbonated lime putty samples L1–L6.

	CRA (BP)	
L1	756	± 16
L2	849	± 17
L3	2658	± 23
L4	132	± 17
L5	140	± 16
L6	198	± 17

be larger than the average binder particles but could be also quite small, close to the size of binder particles. The finest geogenic carbon-bearing particles were not separated by lime putty sedimentation, suggesting that they may not be separable by methods based on mechanical separation (Addis et al. 2019). TA results showed a difference in decomposition temperatures between newly carbonated and geogenic calcites. Although this was determined on fresh partially carbonated quicklime and is not as clearly distinguishable on hardened and aged mortars, the difference in decomposition temperatures can be used to separate geogenic from anthropogenic carbon, which is suitable for the ^{14}C dating (Barret et al. 2021).

CONCLUSIONS

The paper points out that traditional burning in single-batch wood-fired kilns produced highly heterogeneous lime. The assessment by thermal analysis showed that most of the lime could be produced with zero residual geogenic CO_2. However, a certain amount of CO_2 residue should be expected in traditionally produced quicklime. The amount of residual CO_2 is related to the quality of the lime, which is why historical lime processing methods have also minimized unburned particles. Wet slaking of lime in excess water and subsequent storage resulted in settling and sizing. The unburnt particles sank to the bottom of the vessel/lime pit. The practical part of the experiment shows that the way lime was produced and processed is an important factor in the selection of mortar samples for radiocarbon dating. Applications, where a fine binder was required and thus matured in lime pits, are likely to contain little residual geogenic CO_2.

Regarding the assessment methods, the following conclusions can be summarized:

Thermal analysis can be used to differentiate between the newly formed and geologic carbonates in quicklime. Calcium carbonate formed in quicklime decomposes thermally at considerably lower temperatures ($< °C$) than the geogenic carbonate residues present.

Cathodoluminescence proved to be a fast method for assessing the presence of unburned particles even in relatively small quantities. In combination with image analysis, the amount of geogenic contaminants can be quantified by defining the color spectral range. In the case of the six layers examined, image-based CL quantification corresponded to the CO_2 content determined by TA for samples L4–L6 and provided insight into this content in samples L1–L3. For more general use, the quantification procedure should be further developed and verified.

The stable isotope composition of the binder was affected by the fractionation during the reaction and the content of the residual geogenic CO_2. The experiment demonstrated that small amounts of the residual geogenic CO_2, in general isotopically heavier, cannot be distinguished

in the overall composition made of the majority of newly precipitated calcium carbonate. The fractionation of $\delta^{18}O$ and $\delta^{13}C$ by the carbonation reaction absorbing the atmospheric CO_2 of well-burned limes with zero residual geogenic CO_2 was not uniform for the samples from different depth levels of settled and matured lime putty samples. The values $\delta^{13}C$ ranged from –25.5‰ to –20.5‰ VPDB and the $\delta^{18}O$ values ranged from –17.5‰ to –16.5‰ VPDB. The different fractionation was most probably influenced by the character of the portlandite particles, which differed mainly in particle fineness, a parameter that affects the carbonation process. This phenomenon limits the use of stable isotope composition to distinguish small amounts of geogenic contaminants in the newly carbonated lime matrix.

Both, the CL and stable isotope methods proved useful in assessing the particles containing geogenic carbon. Values of $\delta^{13}C \geq$ –20.0‰ VPDB indicate a significant presence of geogenic carbon thus such samples should not be radiocarbon dated without further separation procedures. CL can detect even minor contamination. The image analysis semi-quantitative method has still to be developed further to establish any meaningful limits.

The results of the ^{14}C analysis seem to correlate with the quantified percentage of cathodoluminescent particles. In future experiments, a study involving a statistically larger population will be conducted.

ACKNOWLEDGMENTS

REFERENCES

Adam JP. 1994. Roman buildings: materials and techniques. Routledge.

Addis A, Secco M, Marzaioli F, Artioli G, Arnau AC, Passariello I, Terrasi F, Brogiolo GP. 2019. Selecting the most reliable ^{14}C dating material inside mortars: the origin of the Padua cathedral. Radiocarbon 61(2):375–393.

Barrett GT, Keaveney E, Lindroos A, Donnelly C, Daugbjerg TS, Ringbom Å, Olsen J, Reimer PJ. 2021. Ramped pyroxidation: a new approach for radiocarbon dating of lime mortars. Journal of Archaeological Science 129.

Baxter MS, Walton AF. 1970. Radiocarbon dating of mortars. Nature 225:937–938.

Caroselli M, Hajdas I, Cassitti P. 2020. Radiocarbon dating of dolomitic mortars from the Convent Saint John, Müstair (Switzerland): first results. Radiocarbon 62(3):601–615.

Cazalla O, Rodriguez-Navarro C, Sebastian E, Cultrone G, De la Torre MJ. 2000. Aging of lime putty: effects on traditional lime mortar carbonation. Journal of the American Ceramic Society 83(15):1070–1076.

Daugbjerg TS, Lindroos A, Heinemeier J, Ringbom Å, Barrett G, Michalska D, Hajdas I, Raja R, Olsen J. 2021. A field guide to mortar sampling for radiocarbon dating. Archaeometry 63(5):1121–1140.

Dotsika E, Psomiadis D, Poutoukis D, et al. 2009. Isotopic analysis for degradation diagnosis of calcite matrix in mortar. Anal Bioanal Chem 395:2227–2234.

EN 459-1. 2015. Building lime - Part 1: definitions, specifications and conformity criteria.

Frankeová D, Koudelková V. 2020. Influence of ageing conditions on the mineralogical micro–character of natural hydraulic lime mortars. Construction and Building Materials 264(120205).

Hajdas I, Maurer M, Belen M. 2020. Development of ^{14}C dating of mortars at ETH Zurich. Radiocarbon 62(3):591–600.

Hajdas I, Trumm J, Bonani G, Biechele C, Maurer M, Wacker L. 2012. Roman ruins as an experiment for radiocarbon dating of mortar. Radiocarbon 54(3):897–903.

Hayen R, Van Strydonck M, Fontaine L, Boudin M, Lindroos A, Heinemeier J, et al. 2017. Mortar dating methodology: assessing recurrent issues and needs for further research. Radiocarbon 59(6):1859–1871.

Heinemeier J, Ringbom Å, Lindroos A, Sveinbjörnsdóttir ÁE. 2010. Successful AMS ^{14}C dating of non-hydraulic lime mortars from the medieval churches of the Åland islands, Finland. Radiocarbon 52(1):171–204.

Kosednar-Legenstein B, Dietzel M, Leis A, Stingl K. 2008. Stable carbon and oxygen isotope investigation in historical lime mortar and plaster—results from field and experimental study. Applied Geochemistry 23(8):2425–2437.

Kozlovcev P, Válek J. 2021. The micro-structural character of limestone and its influence on the formation of phases in calcined products: natural hydraulic limes and cements. Materials and Structures 54(6).

Labeyrie J, Delibrias G. 1964. Dating of old mortars by the carbon-14 method. Nature 201:742.

Létolle R, Gégout P, Rafai N, Revertegat E. 1992. Stable isotopes of carbon and oxygen for the study of carbonation/decarbonation processes in concretes. Cement and Concrete Research 22 (2–3):235–240.

Lindroos A, Heinemeier J, Ringbom Å, Braskèn M, Sveinbjörnsdóttir Á. 2007. Mortar Dating Using AMS ^{14}C and sequential dissolution: examples from medieval, nonhydraulic lime mortars from the Aland Island, SW Finland. Radiocarbon 49(1):47–67.

Lindroos A, Ringbom Å, Heinemeier J, Hodgins G, Sonck-Koota P, Sjöberg P, Lancaster L, Kaisti R, Brock F, Ranta H, et al. 2018. Radiocarbon dating historical mortars: lime lumps and/or binder carbonate? Radiocarbon 60(3):875–899.

McCrea JM 1950. On the isotopic chemistry of carbonates and a paleotemperature scale. The Journal of Chemical Physics 18:849–857.

Nawrocka D, Czernik J, Goslar T. 2009. [14]C dating of carbonate mortars from Polish and Israeli sites. Radiocarbon 51(2):857–866.

Oates JAH. 1998. Lime and limestone. Chemistry and technology, production and uses. Weinheim: Wiley-VCH.

Orsowszki G, Rinyu L. 2015. Flame-sealed tube graphitization using zinc as the sole reduction agent: precision improvement of EnvrionMICADAS ^{14}C measurements on graphite targets. Radiocarbon 57:979–990.

Ortega LA, Zuluaga MC, Alonso-Olazabal A, Insausti M, Murelaga X, Ibañez A. 2012. Improved sample preparation methodology on lime mortar for reliable ^{14}C dating. In: Nawrocka DM, editor. Radiometric fating. London: IntechOpen.

Cizer Ö, Rodriguez-Navarro C, Ruiz-Agudo E, Elsen J, van Gemert D, van Balen K. 2012. Phase and morphology evolution of calcium carbonate precipitated by carbonation of hydrated lime. Journal of Materials Science 47:6151–6165.

Pachiaudi C, Marechal J, Strydonck MV, Dupas M, Dauchot-Dehon M. 1986. Isotopic fractionation of carbon during CO_2 absorption by mortar. Radiocarbon 28:691–697.

Ponce-Antón G, Ortega L, Zuluaga M, Alonso-Olazabal A, Solaun J. 2018. Hydrotalcite and Hydrocalumite in mortar binders from the medieval Castle of Portilla (Álava, North Spain): accurate mineralogical control to achieve more reliable chronological ages. Minerals 8(8):326–42.

Ringbom Å, Lindroos A, Heinemeier J, Sonck-Koota P. 2014. 19 years of mortar dating: Learning from experience. Radiocarbon 56(2):619–635.

Ricci G, Secco M, Addis A, Pistilli A, Preto N, Brogiolo GP, Arnau AC, Marzaioli F, Passariello I, Terrasi F, et al. 2022. Integrated multi–analytical screening approach for reliable radiocarbon dating of ancient mortars. Scientific Reports 12(3339).

Stuvier, M, Polach HA. 1977. Reporting of ^{14}C data. Radiocarbon 19(3):355–363.

Stuiver M, Smith C. 1965. Radiocarbon dating of ancient mortar and plaster. In: Olson EA, Chatters RM, editors. Proceedings of the Sixth International Conference Radiocarbon and Tritium Dating. Pullman (WA): Pullman. p. 338–341.

Toffolo BM, Ricci G, Caneve L, Kaplan-Ashiri I. 2019. Luminescence reveals variations in local structural order of calcium carbonate polymorphs formed by different mechanisms. Scientific Reports 9(16170).

Usdowski E. 1982. Reactions and equilibria in the systems CO_2–H_2O and $CaCO_3$–CO_2–H_2O (0–50 °C). Neues Jahrbuch für Mineralogie 144(1982):148–171

Usdowski E, Hirschfeld A. 2000. The $^{13}C/^{12}C$ and $^{18}O/^{16}O$ composition of recent and historical calcite cement and kinetics of CO_2 absorption by calcium hydroxide. Neues Jahrbuch für Mineralogie 11(200):507–521.

Válek J. 2015. Lime technologies of historic buildings. Praha: ÚTAM AV ČR.

Van Strydonck M. 2016. Radiocarbon dating. Topics in Current Chemistry (Z) 374(13).

Wacker L, Christl M, Synal H-A. 2010. BATS: a new tool for AMS data reduction. Nuclear Instruments and Methods in Physics Research Section B 268:976–979.

Wingate M. 1985. Small-scale lime-burning: a practical introduction. London: ITP.